Electrochemical sensor highly selective for lindane determination: a comparative study using three different a-MnO2 nanostructures

Anu Prathap, Mylamparambil Udayan; Sun, Shengnan; Xu, Zhichuan Jason

2016

Anu Prathap, M. U., Sun, S., & Xu, Z. J. (2016). An electrochemical sensor highly selective for lindane determination: a comparative study using three different α-MnO2 nanostructures. RSC Advances, 6(27), 22973-22979.

https://hdl.handle.net/10356/80529

https://doi.org/10.1039/c5ra26771d

RSC Advances

This article can be cited before page numbers have been issued, to do this please use: M.U. A. Prathap, S. Sun and Z. J. Xu, *RSC Adv.*, 2016, DOI: 10.1039/C5RA26771D.

ROYAL SOCIETY OF CHEMISTRY

www.rsc.org/advances

View Article Online
DOI: 10.1039/C5RA26771D

PAPER

Electrochemical sensor highly selective for lindane determination: A comparative study using three different α-MnO_2 nanostructures

Received 00th January 20xx,
Accepted 00th January 20xx

DOI: 10.1039/x0xx00000x

www.rsc.org/

M.U. Anu Prathap, Shengnan Sun, and Zhichuan J. Xu*

Here we describe a simple, highly reproducible ultra-sensitive electrochemical sensor for lindane based on α-MnO_2 nanostructures. The results showed that the α-MnO_2 nanostructures effectively catalyzed the electrochemical reduction of lindane. A good linearity was obtained in the range of 1.1 to 510 μM with a detection limit of 114 nM. The proposed lindane sensor was successfully employed for determining lindane in tap water samples with good recoveries. Negligible amperometric currents are observed in the control experiments using triclosan (T), chlorobenzene (CB), benzene (B), 1,3,5-trichlorobenzene (1,3,5-TCB), and 4-chlorobenzaldehyde (4-CBA), suggesting sensing specificity to lindane. The proposed sensor also exhibited good stability and reproducibility for lindane determination.

Introduction

Lindane (gamma isomer of hexachlorocyclohexane) is an organochlorine insecticide named after Dutch chemist Teunis van der Linden who was the first to isolate α-, β-, and γ-isomers of hexachlorocyclohexane in 1912.[1,2] The insecticidal properties of lindane were first demonstrated by Ulmann, 1972.[1,2] Lindane has been used to treat food crops and to forestry products, as a seed treatment, a soil treatment, and to treat livestock and pets.[1-3] Lindane is reported to be a central nervous system stimulant. Symptoms of acute exposure include mental and motor retardation, central nervous system excitation, tonic-clonic convulsions, respiratory failure, pulmonary edema and dermatitis.[2,3] Lindane enters animal tissues through food chain, respiration or dermal contact.[2,3]After being under review for nearly 30 years, the pesticide lindane was finally withdrawn by the Environmental Protection Agency (EPA) for use in agriculture.[3,4] Lindane is recognized by EPA as one of the most toxic, persistent, bio-accumulative pesticides ever registered.[5] Despite a recent global ban on its agricultural use, the pesticide is still used and approved by the Food and Drug Administration (FDA) as a second-line therapy for topical treatment of pediculosis capitis (head lice), pediculosis pubis (pubic lice), or scabies in patients greater than two years of age who cannot tolerate or have failed first-line treatment.[5] Therefore, quantitative analysis of lindane is a paramount area in the context of the environmental bulwark. New methods, for lindane detection includes more sophisticated analytical approaches, such as gas chromatography, liquid chromatography or gas chromatographic-massspectrometry.[6,7] Although chromatographic methods are accurate, they are expensive and time consuming.[6-8] Among the various biosensing approaches, available to date, electrochemical sensors are emerging to be a technology of choice due to the rapid and sensitive response, low fabrication cost and operational convenience.[7,8] An excellent study discusses the reductive dechlorination of lindane catalyzed by bioreceptor probe.[9] It was found that the specificity of dechlorination depended on the enzyme stability, pH and temperature, which is the major limitation.[7] Lindane has very low aqueous solubility and has a very high overpotential for reduction, as a result the direct reduction of lindane using the aqueous medium is a challenging task. Recent publications discuss on dechlorination of lindane in ethanol/water and lindane gave only one reduction wave and benzene as the reduction product with 100 % yield.[10-15] The results of other researchers show chloride ion was liberated from lindane structure more rapidly than hydrogen or carbon atom fragments.[10-15] Few studies have been dedicated to the non-enzymatic sensing of lindane using metal oxide, and it appears to be more effective.[12,15] Thus, it is important to pursue a suitable modified electrode for the efficient reduction of lindane.

In recent years, the application of nanoscaled metal oxides has received great attention in biotechnology and bio-analytical chemistry.[16-20] Transition metal element; manganese can exist as a variety of stable oxides (MnO, Mn_3O_4, Mn_2O_3, MnO_2) and crystallize in various types of crystal structures. Among them, α-MnO_2 has been widely investigated and extensively used in adsorption, catalysis, sensors, rechargeable lithium batteries

School of Materials Science and Engineering, Nanyang Technological University, 50 Nanyang Avenue, Singapore 639798, Singapore. E-mail: xuzc@ntu.edu.sg
†*Electronic Supplementary Information (ESI) available: [Experimental details, supplementary figures]. See DOI: 10.1039/x0xx00000x*

View Article Online
DOI: 10.1039/C5RA26771D

and ion exchanges owing to the existing unique layers or tunnels in crystal lattices.[21-23] It is generally accepted that the physicochemical properties of MnO_2 are greatly affected by the crystallographic structure, morphology, and surface area.[21]

In this work, we report three synthetic pathways for the preparation of α-MnO_2 nanostructures, (e.g., NW (nanowire), NT (nanotube), and MS (microsphere); designated as: α-MnO_2-NW, α-MnO_2-NT, and α-MnO_2-MS). We further demonstrated α-MnO_2 nanostructures exhibit excellent electrocatalytic activity for lindane reduction. The prepared sensor was characterized by electrochemical impedance spectroscopy (EIS), differential pulse voltammetry (DPV), cyclic voltammetry (CV), pulsed amperometry (PA) and chronoamperometry. Under the optimized conditions, the prepared sensor exhibited selective recognition and a highly sensitive detection toward lindane.

Experimental

Materials

All chemicals were analytical grade and used without further purification. $KMnO_4$, urea, γ-HCCH (Lindane), cyclohexane, chlorobenzene, 4-chlorobenzaldehyde, triclosan, benzene and tetra-n-butyl ammonium bromide (TBAB) were obtained from Sigma-Aldrich. Deionized water from Millipore Milli-Q system (Resistivity 18.2 MΩ cm) was used in the electrochemical studies. Solutions for all electrochemical experiments were deoxygenated with zero-grade argon.

Preparation of solution

Stock solution of lindane was prepared in methanol. 0.05 M tetra-n-butyl ammonium bromide (TBAB) solution was prepared in 60:40 (v/v) methanol–water. It was used as the supporting electrolyte.

Synthesis of α-MnO_2 microspheres (α-MnO_2-MS)

α-MnO_2-MS was synthesized by a hydrothermal approach with a modified procedure first reported by our group.[15] 1.5 mmol (0.237 g) of $KMnO_4$ was dissolved in 100 mL of deionized water (DW), followed by the addition of 5 mL hydrochloric acid (11.65 M, 35% (w/w)), forming a solution. The resulting mixture was stirred for 0.5 hr; the solution was transferred to a Teflon-lined autoclave (50 mL capacity). The hydrothermal process was conducted at 353 K for 12 hr. Product was filtered, washed with water and ethanol, dried in an oven at 353 K for 8 h.

Synthesis of α-MnO_2 nanowires (α-MnO_2-NW)

α-MnO_2-NW was prepared by reported procedure with increased temperature for higher purity samples.[24] In a typical procedure, 10 mmol (0.6 gram) of urea was dissolved in 35 mL deionized water, followed by the addition of 10 mmol (1.58 g) $KMnO_4$, forming a solution. The resulting mixture was stirred for 30 min; the solution was transferred to a Teflon-lined autoclave (50 mL capacity). The hydrothermal process was conducted at 433 K for 20 hours. The products was filtered, washed with DW and dried at 353 K overnight.

Synthesis of α-MnO_2 hollow nanotube (α-MnO_2-NT)

α-MnO_2-NT was synthesized by a hydrothermal approach by modifying the recipe.[25] 15 mmol (2.37 g) of $KMnO_4$ was dissolved in 200 mL of deionized water (DW), followed by the addition of 5 mL hydrochloric acid (11.65 M, 35% (w/w)), forming a solution. The resulting mixture was stirred for 0.5 hr; the solution was transferred to a Teflon-lined autoclave (50 mL capacity). The hydrothermal process was conducted at 383 K for 15 hr. Product was filtered, washed with water and ethanol, dried in an oven at 353 K for 8 h.

Materials characterizations

The as-prepared materials were characterized with X-ray powder diffractometer (XRD; Shimadzu XRD-6000, Cu Kα radiation) at a scan rate of 1° min^{-1}. Scanning Electron Microscopy (FESEM, JSM-7600F) and transmission electron microscopy (TEM; JEOL, JEM-2100F) operated at 200 kV was used to observe the morphological features. Nitrogen adsorption measurement at 77 K was performed by Tristar-3000 surface area analyzer. Samples were out-gassed at 423 K for 4 h in the degas port of the adsorption apparatus. The specific surface area was determined by Brunauer–Emmett–Teller (BET) method using the data points of P/P_0 in the range of about 0.05–0.3.

Electrochemical measurements

Cyclic voltammetry (CV), Differential pulse voltammetry (DPV), Pulsed amperometry (PA) and Continuous amperometric studies were performed by using a computer-controlled Pine Instrument. A three electrode electrochemical cell was employed with Ag/AgCl as the reference electrode (3M KCl), metal oxide mounted glassy carbon electrode (GCE) (0.196 cm^2) as the working electrode, and Pt foil as the counter electrode. Before modification of GCE, the polished electrode was ultrasonicated in ethanol and deionized water for 5 minutes, respectively. The working electrodes were prepared as follows: 10 μL aliquot of MnO_2 suspension (a homogenous sonicated solution of 10 mg of MnO_2 and a mixture of 0.1 mL of Nafion and 0.9 mL of water) was placed onto the electrode surface, the electrode was dried in air leaving the material mounted onto the GCE surface.

Results and discussion

XRD analysis was primarily used to determine the structure of the α-MnO_2-NW (Fig. 1a). All the diffraction peaks can be indexed to a tetragonal α-MnO_2 (JCPDS, file No.: 44-0141). Similar XRD observation was also noticed for α-MnO_2-NT and α-MnO_2-MS prepared in this study (Figure not shown). Fig. 1b-h shows the SEM and HRTEM images with different magnifications of α-MnO_2-MS, α-MnO_2-NT, and α-MnO_2-NW. The SEM morphology of α-MnO_2-MS is spherical with a flower-like morphology (Fig. 1b,c). The higher magnification image shows that the petal structure of microspheres is assembled by many nanosheets (Fig. 1c). Figs. 1(d-f) is the representative SEM and HRTEM images of the as-prepared α-MnO_2-NT. Evidently, each MnO_2 nanotubes are of high quality; they are open-ended and have a length of hundreds of

View Article Online
DOI: 10.1039/C5RA26771D

nanometer Figs. 1(e,f). Fig. 1g shows the low magnification SEM image of the α-MnO_2-NW; it can be found that the product consists of nanowires. The MnO_2 nanowires are further investigated by HRTEM (Fig. 1h). The diameters of the presented MnO_2 nanowire are within 50 nm (Fig. 1h). The N_2 sorption isotherm of the α-MnO_2-NW sample shows a type IV curve with a sharp capillary condensation step in the relative pressure range of 0.6–1 and H_1 hysteresis loop, indicative of uniform cylindrical mesopores (Fig. 2a).[26] α-MnO_2-NT nanostructures synthesized in this study exhibited type IV isotherm with H_3 hysteresis, which is characteristic of the mesoporous materials. High uptake of N_2 adsorption at a low relative pressure (~ 0.4) reveal abundant micropores located in the α-MnO_2-NT (Fig. 2a). Textural properties for various materials obtained from the N_2-adsorption study is provided in Table S1, ESI†. The specific BET surface area for α-MnO_2-NW, α-MnO_2-NT, and α-MnO_2-MS were found to be 124.2 m^2/g, 79.3 m^2/g and 12.2 m^2/g, respectively. From the SEM images it can be seen that α-MnO_2-NW has short fiber lengths and diameters ~ 50 nm, while α-MnO_2-NT has a diameter of ~ 110 nm and α-MnO_2-MS has higher diameter (sub-micrometer size), the decrease of the lateral dimensions (diameter) to the nanoscale offers a high specific surface area and a high surface site density to α-MnO_2-NW (Fig. 1).[26]

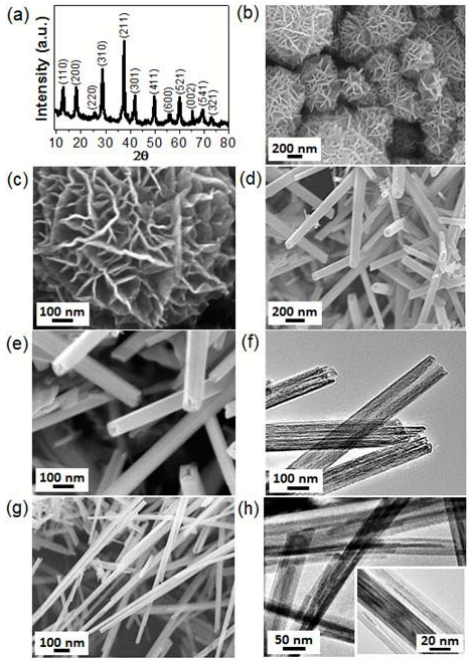

Fig.1 XRD pattern (a) of α-MnO_2-NW. FE-SEM images (b,c) of α-MnO_2-MS, FE-SEM images (d,e) and TEM image (f) of the α-MnO_2-NT, and FE-SEM image (g) and TEM images (h) of the α-MnO_2-NW. The inset of (h) is a close view of α-MnO_2-NW.

The electrochemical behavior of different modified electrodes was investigated using potassium ferricyanide as the electrochemical probe by CV. Study was performed in 0.2 M KCl solution containing 50 mM $K_3[Fe(CN)_6]/K_4[Fe(CN)_6]$ at a scan rate of 20 mV/s at different modified electrodes. The CV of various modified electrodes exhibited a pair of well-defined redox peaks corresponding to $Fe(CN)_6^{3-/4-}$ redox couple (Fig. 2b). Among the various modified electrodes investigated in this study, α-MnO_2-NW exhibited the highest current response. The electroactive surface area of various electrodes was calculated according to the Randles-Sevčik equation (Eq. 1).[23]

$$I_p = (2.69 \times 10^5)\, n^{3/2}\, AD^{1/2}\, C\, v^{1/2} \qquad (1)$$

Where, I_p is the peak current of redox couple, n is the number of electrons participating in the redox reaction, A is the electroactive surface area (cm^2), D is the diffusion coefficient of $K_3[Fe(CN)_6]$ in the solution (cm^2/s), C is the concentration of $K_3[Fe(CN)_6]$ in the bulk solution (mol/cm^3), and v is the scan rate (V/s). The effective surface area of different modified electrodes was calculated as 0.403, 0.305, and 0.259 cm^2 for α-MnO_2-NW, α-MnO_2-NT, and α-MnO_2-MS, respectively. The high electroactive surface area of α-MnO_2-NW significantly eases the electron transfer rate at the electrode-electrolyte interface.[27] Fig. 2c displays typical Faradaic impedance spectra (presented as Nyquist plot) of the α-MnO_2-NW electrode before and after additions of different concentrations of the lindane. Electrochemical impedance spectra were recorded in the frequency range from 1 MHz to 10 mHz with the AC signal amplitude of 10 mV. It can be clearly observed that the electron-transfer resistance (semicircle diameter) decreases as the lindane concentration is elevated. In EIS, the diameter of the semicircle portion at higher frequencies corresponds to the electron-transfer resistance (R_{et}). The change of R_{et} value at high frequencies was associated with the blocking behavior of the modified layer at the electrode surface.[28] The collected data show that the R_{et} values are significantly smaller after the addition of lindane, e.g., decreasing from 7.02 kΩ to 3.12 kΩ, upon increasing the lindane concentration from 0 to 180 μM. The smaller semi-circle diameter (i.e. lower value of R_{et}) indicates faster electron-transfer kinetics of lindane (reduction) at the α-MnO_2-NW modified electrode.[28]

α-MnO_2-NW modified electrode was constructed to obtain the optimized analysis parameter for lindane reduction. The electrochemical behaviour of lindane was first investigated using cyclic voltammetry in the absence and presence of 300 μM lindane. In the absence of lindane, no peak was observed. When lindane was added, a distinct peak at –1.45 V (versus Ag/AgCl) was appeared, which is completely irreversible (Fig. S1, ESI†).[10-15] The effect of scan rate (range of 20–200 mV s^{-1}) was investigated to predict the reaction kinetics process using cyclic voltammetry as shown in Fig. 2d. The results reveal that the reduction peak current of lindane was directly proportional to the square root of scan rate up to 200 mV s^{-1}, the negative intercept suggests that the electrode reaction is not a pure diffusion-controlled process (Fig. 2d, inset).[10-15] Randles-Sevčik equation for a reduction process with a zero intercept suggests a complete diffusion control process, thus, the negative intercept from the plot of peak current versus square root of scan rate can be explained as an adsorption of the lindane molecule after diffusion to the electrode surface.[15] The results of the voltammetric analyses are collected in Table S2. The electron transfer coefficient α was calculated from the peak width ($\Delta E_{p/2} = E_{p/2} - E_p$). For all scan rates, a very low value of α is obtained less than 0.5, showing that the rate-determining

View Article Online
DOI: 10.1039/C5RA26771D

step of the electrode process is dissociative electron transfer (ET), which is concerted with the cleavage of the carbon–halogen bond.[29,30] Dechlorination or displacement of chlorine of polychlorinated cyclohexanes is different from the dechlorination of polychlorinated benzenes.[31,32] Earlier workers reported that the elimination of a chlorine atom by the reduction of polychlorinated benzenes always leads to a product that is more difficult to be reduced.[30,31] In contrast, breaking of carbon-chlorine bonds in lindane occur very fast and readily form fully reduced benzene.[31,32]

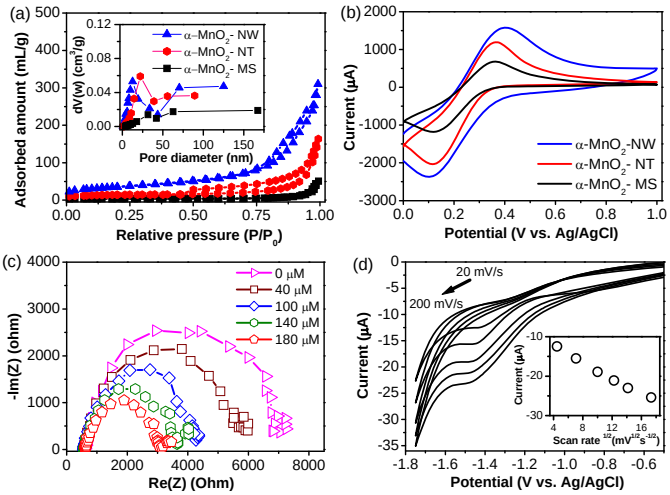

Fig. 2 (a) N_2 adsorption–desorption isotherms of materials synthesized in this study. The inset shows pore size distribution. (b) CV responses of various modified electrodes in 0.2 M KCl electrolyte containing 50 mM of $[Fe(CN)_6]^{3-/4-}$ at a scan rate of 20 mVs^{-1}. (c) Typical EIS response recorded at the α-MnO_2-NW modified electrode in the presence of increasing concentrations of lindane, using 0.05 M TBAB solution in 60:40 methanol–water (20 mL) over the frequency range from 1 MHz to 10 mHz a bias potential of -1.45 V. (d) CVs of lindane (200 μM) at various scan rates (20-200 mVs^{-1}) at α-MnO_2-NW modified electrode. Inset shows the plot of peak currents vs. square root of scan rates. All scans are applied between -0.6 V and -1.8 V.

Under the optimized conditions, pulsed amperometry and differential pulse voltammetry were used to determine lindane concentration. The Fig. 3a shows the pulsed amperometric response of α-MnO_2-NW modified electrode to lindane. At the constant potential -1.45 V (*vs* Ag/AgCl), the measured current response is linear vs. the lindane concentration (Fig. 3a). α-MnO_2-NW modified electrode can detect lindane in the concentrations range from 1.1 to 510 μM in the amperometric mode with a linear regression equation of, $I(\mu A)$ = -4.64-0.0346C (μmol L^{-1}) (R^2 = 0.9989) with the sensitivity of 0.18 μA μM^{-1} cm^{-2} and a lower detection limit of 114 nM. The intercept of the calibration curve was not found to be zero, suggesting undesired non-Faradaic processes (Fig. 3a, inset).[33] DPV measurements were also carried out containing different lindane concentrations to obtain an analytical curve. Fig. 3b shows that the cathodic peak current was linearly dependent on the lindane concentration in the range from 2 to 520 μM with a linear regression equation of, $I(\mu A)$ = -6.208-0.022C (μmol L^{-1}) (R^2 = 0.9983) with the sensitivity of 0.14 μA μM^{-1} cm^{-2} and a lower detection limit of 517 nM (Fig. 3b, inset). Similarly, linear relationship between oxidation peak currents and lindane concentrations was observed in the range of 4–500 μM, and 15–350 μM for α-MnO_2-NT and α-MnO_2-MS modified electrodes (Fig. S2 and Fig. S3, ESI†). To obtain the limit of detection (LOD), we used an IUPAC (International Union of Pure and Applied Chemistry) recommended methodology, using the standard approach of alternative (SA).[34]

$$LOD_{SA} = 3S/q \qquad (2)$$

Where S is the standard deviation of the blank signal, and q is the slope of the calibration curve. A comparison of the modified electrodes toward electrocatalytic reduction of lindane is presented (Fig. 4a). Based on the experimental evidence, one can conclude that α-MnO_2-NW modified electrode exhibited superior sensing ability and current sensitivity compared to other modified electrodes investigated in this study. The high electrocatalytic response observed for the α-MnO_2-NW can be correlated with the large surface area, excellent site accessibility and a low mass-transfer resistance for lindane.

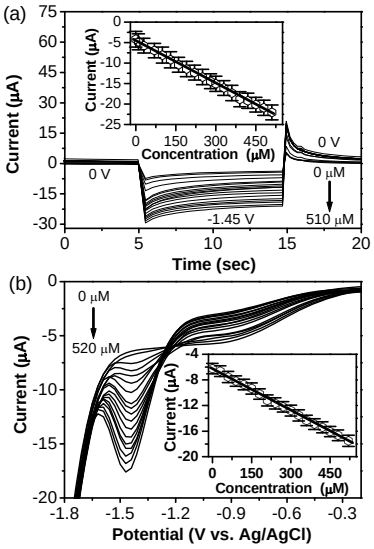

View Article Online
DOI: 10.1039/C5RA26771D

Fig. 3 (a) Pulsed amperometric response of the α-MnO_2-NW modified electrode to different concentrations of lindane at the specified voltage values. The inset shows the calibration plot. (b) DPVs of lindane at varying the concentrations at the α-MnO_2-NW modified electrode using 0.05 M TBAB solution in 60:40 methanol–water (20 mL). The inset shows the calibration plot. DPV parameters were selected as: peak height = 50 mV; peak width = 200 ms; peak period = 400 ms; increment = 20 mV; pre and post-pulse width = 3 ms.

The sensing ability of the prepared α-MnO_2-NW modified electrode towards lindane was compared with the reported nanostructures (Table S3, ESI†).[9,12,13,15,35-37] The performance of α-MnO_2-NW nanostructures modified electrode is comparable if not superior to those reported in the literature Table S3, ESI†. For the practical use of non-enzymatic lindane sensors, specificity is another important factor that needs attention. Under a rational design, the designed lindane sensor should have minimal interferences from water and soil samples from industrial areas and agricultural land. In the present work, interfering compounds were picked based on structural similarity and solubility in water and soil.[37-39] Therefore, inorganic ions, electroactive organic compounds and organic compounds containing chlorine groups were chosen which may potentially interfere with determination of lindane.[37-39] The amperometric response of the α-MnO_2-NW modified electrode to the stepwise addition of lindane in the presence of 1 mM each of various interfering species such as cyclohexane (CH), triclosan (T), chlorobenzene (CB), and benzene (B) at an applied potential of -1.45 V is shown in Fig. 4b. The α-MnO_2-NW modified electrode shows excellent anti-interference behaviour towards interfering species (Fig. 4b). It may further be noted that when 150 times higher concentration of 4-CBA (0.5 M) and 1,3,5-TCB (0.5 M) interfere with the determination of lindane (Fig. 5(a,b)). The results also showed that 1 mM concentrations of inorganic ions (Ca^{2+}, Co^{2+}, Mg^{2+}, Mn^{2+}, Ni^{2+}, and Zn^{2+}) did not interfere with the detection of lindane (Fig. 5c).

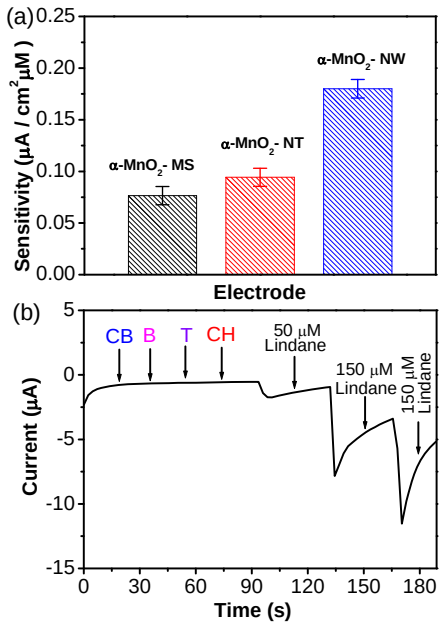

Fig. 4 (a) Comparison of the sensitivity for lindane at different modified electrodes investigated in this study. (b) Continuous amperometric response at the α-MnO_2-NW modified electrode in the presence of high concentration of interfering species, such as chlorobenzene (1 mM), benzene (1 mM), triclosan (1 mM), and cyclohexane (1 mM) as compared to the successive addition of lindane.

Fig. 6a illustrates a pulse amperometric response for series of injections of standard lindane solution at a fixed potential (pulse sequence (n)=5). Fig. 6a shows that when a fixed potential was applied (-1.45 V) the signal current increased relatively fast and no decrease of the signal was observed during the pulse length (relative standard deviation ~ 1.02%), suggesting very high reproducibility. After each measurement, the electrode was rinsed thoroughly with deionized water and was stored at room temperature when not in use and reactivated by dipping in the supporting electrolyte for 30 minutes before measurement. Furthermore, α-MnO_2-NW modified electrode could be used more than 13 times after subsequent cycles of washing and measuring operations. On the other hand, three fresh fabricated α-MnO_2-NW modified electrodes were also used for determining 50 μM lindane. The RSD was calculated to be 2.71%. Therefore, our proposed lindane electrochemical sensor has a satisfactory repeatability. We examined the current stability for α-MnO_2-NW modified electrode by recording amplitude of the pulse currents correspond to the addition of lindane (200 μM) (Fig. 6b). The amplitude of the 40 pulse currents display insignificant changes (<0.5%), indicating a good stability of the α-MnO_2-NW modified electrode. The storage stability was tested by storing the α-MnO_2-NW modified electrode for two weeks. The result showed that the reduction peak potential of lindane had no shift and the current response only showed 4.3% decrease compared with the original test.

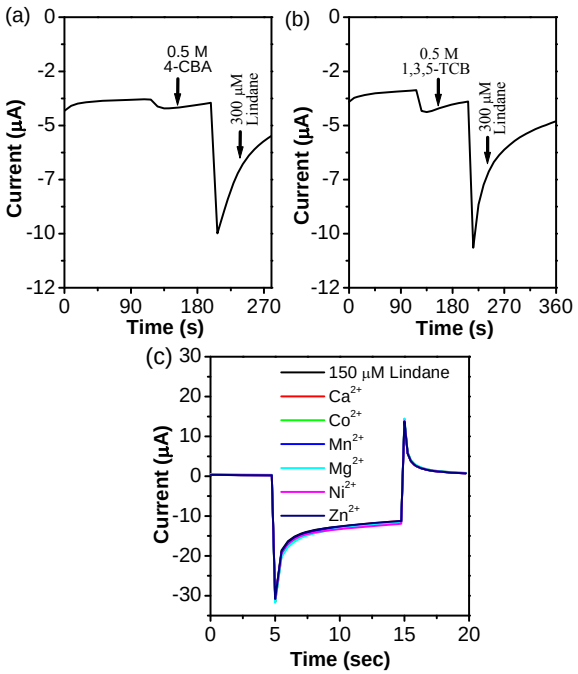

Fig. 5 Continuous amperometric response at the α-MnO_2-NW modified electrode in the presence of high concentration of interfering species, such as (a) 4-chlorobenzaldehyde (0.5 M), and (b) 1,3,5-trichlorobenzene (0.5 M) as compared to the addition of lindane (300 μM). (c) Pulsed amperometric response to 150 μM lindane spiked with 1mM each of various metal ions at α-MnO_2-NW modified electrode (E_1 = 0 V for 5 s; E_2 = -1.45 V for 10 s and E_3 = 0 V, for 5 s).

View Article Online
DOI: 10.1039/C5RA26771D

To demonstrate the feasibility of sensor in practicable application, the proposed sensor was applied to the determination of lindane in tap water samples. No voltammetric response corresponding to lindane was observed in tap water, thus different quantity of lindane was added to the tap water samples. Spiking method was adopted to evaluate the lindane content of three samples. The standard addition methodology was used to determine the average recovery of lindane as well as to validate the proposed method. The results were summarized in Table S4, ESI†. As can be seen from Table S4, ESI†, the recoveries were from 98.5% to 102.0%. The recovery calculations indicated the potential practical application of our proposed sensor.

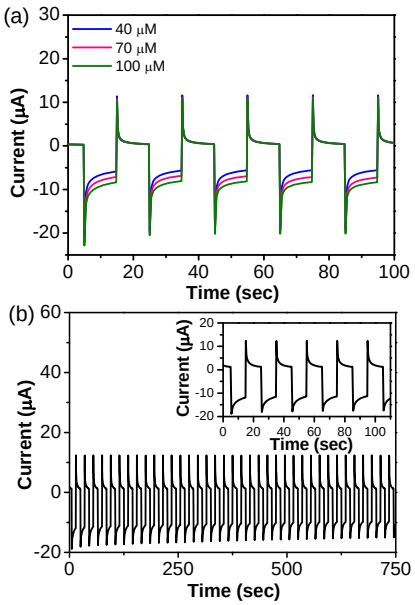

Fig. 6 (a) Pulsed amperometric response (n = 5) of the α-MnO_2-NW modified electrode to increasing concentration of lindane (E_1 = 0 V for 5 s; E_2 = -1.45 V for 10 s and E_3 = 0 V, for 5 s). (b) Pulsed amperometric response (n = 40) of the α-MnO_2-NW modified electrode to 200 μM of lindane (E_1 = 0 V for 5 s; E_2 = -1.45 V for 10 s and E_3 = 0 V, for 5 s). The inset shows an enlarged view (n=5).

Conclusions

In summary, we demonstrate a novel electrocatalyst for the non-enzymatic reduction of lindane based on α-MnO_2 nanostructures. The sensors fabricated from the α-MnO_2-NW exhibited the highest performance among the studied materials with lower detection limit, high sensitivity, and wide linear range, making this novel sensing methodology an extremely promising one. We envision that this methodology reported here for the lindane reduction recommends a broad research in that direction.

Acknowledgements

This work was supported by MOE Tier 1 Grants (RGT8/13 and RG131/14) of Singapore and the Singapore National Research Foundation under its Campus for Research Excellence And Technological Enterprise (CREATE) programme. Authors thank the Facility for Analysis, Characterisation, Testing and Simulation (FACTS) in Nanyang Technological University for materials characterizations.

Notes and references

1 C. L. Willett, E. M. Ulrich and R. A. Hites, *Environ. Sci. Technol.*, 1998, **32**, 2197.
2 A. J. Durie, A. M. Z. Slawin, T. Lebl and D. O' Hagan, *Angew. Chem. Int. Ed.,* 2012, **51**, 10086.
3 T. M. Phillips, A. G. Seech, H. Lee and J. Trevors, *Biodegradation*, 2005, **16**, 363.
4 B. R. Garrido, T. A. L. Chau, G. Feijoo, F. Macias and M. C. Monterrroso, *Environ. Sci. Technol.*, 2010, **44**, 7063.
5 S. Li, D. W. Elliott, S. T. Spear, L. Ma and W. -X. Zhang, *Crit.Rev. Environ. Sci. Technol.*, 2011, **41**, 1747.
6 S. L. Simonich and R. A. Hites, *Science*, 1995, **269,** 1851.
7 M. Oturan, N. Oturan, C. Lahitte and S. Trevin, *J. Electroanal. Chem.*, 2001, **507**, 96.
8 G. Liu and Y. Lin, *Anal. Chem.*, 2005, **77**, 5894.
9 M. U. Anu Prathap, A. K. Chaurasia, S. N. Sawant and S. K. Apte, *Anal. Chem.,* 2012, **84,** 6672.
10 J. P. Merz, B. C. Gamoke, M. P. Foley, K. Raghavachari and D. G. Peters, *J. Electroanal. Chem.* 2011, **660**, 121.
11 A. A. Peverly, J. A. Karty and D. G. Peters, *J. Electroanal. Chem.* 2013, **692**, 66.
12 M. U. Anu Prathap and R. Srivastava, *Electrochim. Acta*, 2013, **108**, 145.
13 A. Kumaravel, S. Vincent and M. Chandrasekaran, *Anal. Methods,* 2013, **5**, 931.
14 P. R. Birkin, A. Evans, C. Milhano, M. I. Montenegro and D. Pletcher, *Electroanalysis,* 2004, **16**, 583.
15 M. U. Anu Prathap, S. Sun, C. Wei and Z. J. Xu, *Chem. Commun.*, 2015, **51**, 4376.
16 J. F. Rusling, T. F. Connors, and A. Owlia, *Anal. Chem.*, 1987, **59**, 2123.
17 H. B. Wu, J. S. Chen, H. H. Hng and X. W. D. Lou, *Nanoscale*, 2012, **4**, 2526.
18 M. U. Anu Prathap, and R. Srivastava, *Sens. Actuators, B,* 2013, **177**, 239.
19 M. U. Anu Prathap, and R. Srivastava, *Nano Energy*, 2013, **2**, 1046.
20 M. U. Anu Prathap, B. Kaur and R. Srivastava, *J. Colloid Interface Sci.*, 2012, **381**, 143.
21 C. Chen, Q. Xie, D. Yang, H. Xiao, Y. Fu, Y. Tan and S. Yao, *RSC Advances*, 2013, **3**, 4473.
22 C. Wei, L. Yu, C. Cui, J. Lin, C. Wei, N. Mathews, F. Huo, T. Sritharan and Z. Xu, *Chem. Commun.*, 2014, **50**,7885.
23 M. U. Anu Prathap, V. Anuraj, B. Satpati and R. Srivastava, *J. Hazard. Mater.*, 2013, **262,** 766.
24 X. C. Duan, J. Q. Yang, H. Y. Gao, J. M. Ma, L. F. Jiao and W. J. Zheng, *CrystEngComm*, 2012, **14**, 4196.
25 J. Luo, H. T. Zhu, H. M. Fan, J. K. Liang, H. L. Shi, G. H. Rao, J. B. Li, Z. M. Du, Z. X. Shen, *J. Phys. Chem. C,* 2008, **112**, 12594.
26 L. Qian, L. Gu, L. Yang, H. Y. Yuan and D. Xiao, *Nanoscale*, 2013, **5**, 7388.
27 Y. Wang, Y. Zhu, J. Chen and Y. Zeng, *Nanoscale*, 2012, **4**, 6025–6031.
28 M. C. Rodriguez, A. N. Kawde and J. Wang, *Chem. Commun.*, 2005, 4267.
29 A. A. Isse, L. Falciola, P. R. Mussini and A. Gennaro, *Chem. Commun.,* 2006, 344.
30 A. A. Isse, S. Gottardello, C. Durante and A. Gennaro, *Phys. Chem. Chem. Phys.,* 2008, **10**, 2409.
31 D. G. Peters, in *Organic Electrochemistry*, ed. H. Lund and O. Hammerich, Marcel Dekker, New York, 4th edn., 2000, ch. 8, pp. 341–377.

View Article Online
DOI: 10.1039/C5RA26771D

32 S. M. Kulikov, V. P. Plekhanov, A. I. Tsyganok, C. Schlimm and E. Heitz, *Electrochim. Acta* 1996, **41**, 527.
33 E. Grygolowicz-Pawlak and E. Bakker, *Electrochem. Commun.*, 2010, **12**, 1195.
34 J. Mocak, A. M. Bond, S. Mitchell and G. Scollary, *Pure Appl. Chem.*, 1997, **69**, 297.
35 P. Wang, L. Ge, M. Li, W. Li, L. Li, Y. Wang and J. Yu, *J.Inorg.Organomet.Polym.*, 2013, **23**, 703.
36 P. R. Birkin, A. Evans, C. Milhano, M. I. Montenegro and D. Pletcher, *Electroanalysis*, 2004, **16**, 583.
37 T. S. Anirudhan and S. Alexander, *Biosens. Bioelectron.*, 2015, **64**, 586.
38 I. Ali and C. K. Jain, *J. Environ. Hydrol.*, 2001, **9**, 1.
39 C. Xu, K. Wu, S. Hu and D. Cui, *Anal. Bioanal. Chem.*, 2002, **373**, 284.

View Article Online
DOI: 10.1039/C5RA26771D

TOC